Kurdish Studies
July 2024
Volume: 12, No: 5, pp 857-864
ISSN: 2051-4883 (Print) | ISSN 2051-4891 (Online)
www.KurdishStudies.net

DOI:10.53555/ks.v12i5.3367

Green Synthesis of Zinc Oxide Nanoparticles Using Aqueous Extract from *Pinus Roxburghii* (L.)leaves

Khadija Kiran[1]*, Asma Ahmed[1], Hasan Akbar Khan[2], Khalil Ali[3], Muhammad Nadir Habib[1], Saad Ahmed Khan[1]

[1]*Institute of Molecular Biology and Biotechnology, The University of Lahore, Lahore - Pakistan
[2]Department of Biochemistry, Al-Aleem Medical College, Lahore - Pakistan.
[3]Department of Biological Sciences, Superior University Lahore, Lahore - Pakistan

***Corresponding Author:** Khadija Kiran
*Institute of Molecular Biology and Biotechnology, The University of Lahore, Lahore – Pakistan

ABSTRACT
Zinc oxide nanoparticles (ZnO) were synthesized using aqueous leaf extract of *Pinus roxburghii* L. (Chir) via green synthesis as due to least toxic effect on environment, green synthesis has become one of the most important methods for the synthesis of particles at nanoscale. Ultraviolet- Visible (UV-Vis) spectrum was used to assess the size of synthesized nanoparticles, XRD and SEM analysis was further used to confirm the exact size and shape of these green nanoparticles, while functional groups were recorded by using FTIR analysis. Change in color of the reaction mixture (pale yellow to whitish) was the visual confirmation of ZnO particles while UV- Vis analysis presented a sharp peak at 377 nm which confirmed that the synthesized particles were in nanoscale range. Hexagonal wurtzite structure of ZnO nanoparticles was confirmed through XRD analysis which gives distinct peaks at 2θ position. The average size of nanoparticles was around 24.71 nm with irregular shape of particles. Leaf extract of *P. roxburghii* L. was found excellent reducing agent for the synthesis zinc oxide nanoparticles.

Key words: *Pinus roxburghii* L., Zinc nanoparticles, XRD, FTIR and SEM.

INTRODUCTION
Nanotechnology is a field of science dedicated to the design, synthesis, characterization and application of materials and devices on nanometer scale. That is less than 100 nanometers. Which is about 1000 times smaller than width of a human hair. Ability of nanotechnology to create materials and devices with novel properties is a great platform for innovation and advancement. By controlling synthesis of materials at tiny or minute dimensions with specific shape, size and properties help researchers develop novel materials with revolutionary properties (Divya et al., 2018). Nanotechnology is a key driver of innovations across many fields such as physics, biology, chemistry and materials science (Karthika et al., 2017). Nanoparticles have wide-ranging applications across multiple industries such as medicine, drug delivery, diagnostics, agriculture, environment and materials science. Manipulation of materials at nanoscale opens up possibilities improving health, advancing technology, addressing environmental challenges and enhancing everyday products (Benelli et al., 2018). Application of nanotechnology in agriculture offers innovative solutions to some of the most pressing challenges in farming such as nutrient delivery, pest control and sustainable practices (Badar et al., 2023).
Synthesis of nanoparticles is a foundational aspect of nanotechnology, and various methods have been developed to create nanoparticles with specific shape, size and properties. These methods are physical, chemical and biological (Ishwarya et al., 2018). Physical methods involve breaking down bulk materials into nanoscale particles. Chemical methods involve assembly of nanoparticles from atomic or molecular precursors. Biological methods involve green synthesis of nanoparticles (Banumathi et al., 2017). This eco-friendly approach uses plants or microorganisms for synthesis of nanoparticles (Singh et al., 2017). Ongoing research in this area focuses on improving synthesis techniques to achieve greater control over particle size, shape and surface chemistry, while also addressing concerns related to environmental impact and sustainability. As techniques continue to advance, the potential for nanoparticles to revolutionize fields such as medicine, energy and environmental science will only grow.
Most important feature of nanoparticles is, as their size decreases, the surface to volume ratio increases significantly. This property makes nanoparticles more reactive allowing for more interactions with surrounding environments. High surface to volume ratio allows for the efficient attachment of the drugs to the surface of nanoparticles. This enables targeted delivery of therapeutic agent to specific cells or tissues, such as cancer cells, while minimizing side effects (Mundekkad et al., 2022). Due to their enhanced reactivity, nanoparticles are widely used as catalyst for production of chemicals, pharmaceuticals and energy conversion process (Narayan et al., 2019). High surface area of nanoparticles is utilized in formulation of nanofertilizers and pesticides (Neme et al., 2021).
The conventional physical and chemical methods of nanoparticles synthesis have many disadvantages such as high cost, less environment friendly and health risks. Green synthesis of nanoparticles is environment friendly and sustainable. Green

synthesis occurs under mild conditions such as room temperature and atmospheric pressure and these nanoparticles are biocompatible which is advantageous for medical and environmental application ((Sharma et al., 2021).
Based on better pharmacodynamics, improved safety, and nutritional productiveness, bioactive compounds of plants are getting immense limelight.Plants have been used for centuries in traditional medicine to treat various diseases (Jakaria et al., 2017). Some of these plants have been directly used in medicines while others have led to the development of modern drugs (Bisht et al., 2019).
Pinus roxburghii L. is native to the Himalayan region (Secim-Karakaya et al., 2021). In Pakistan, it is found in Azad Kashmir, Khyber Pakhtunkhwa, and some parts of Punjab (Shankar et al., 2015). Documented roles of *P. roxburghii* L. are anticancer (Sajid et al., 2018), antiparasitic (Farooq et al., 2008), antimicrobial (Salem et al., 2014), antihyperlipidemic (Safaeian et al., 2019), anti-inflammatory (Labib et al., 2017) and antioxidant (Sharma et al., 2020).
P. roxburghii L. is commonly known as Chir, Chil and is enriched source of B-secretase 1 and cholinesterase, pinene, flavoanoids, which have strong Anti-inflammatory, anticancer, antioxidant activities (Bhardwaj et al., 2022; Hou et al., 2019).

Methodology

Experimental plant

Plant was collected in triplicates from Minimerg, Pakistan (34.7908°N 75.0799°E), stored at -80 °C to prevent stress, identified by informed taxonomists for voucher number at Department of Botany, Government College University, Lahore, and preserved at the University of Lahore, Lahore, with their botanical numbers.

Preparation of Leaf Extract

Collected leaves of *P. roxburghii* L. were carefully washed and dried to remove the excess moisture, which were then ground to make fine powder and sieved. Boil five grams of the powder in100ml of distilled water at 60 ℃ for 2 hours. Filter the mixture using filter paper.

Preparation of 1.0 M Zinc chloride

For the synthesis of zinc oxide nanoparticles, 20 ml of filter solution were taken in 250 ml volumetric flask at 70 °C. Reaction mixture was covered with aluminum foil, this reaction was sustained for 2.0 hours, with constant stirring during the reaction to ensure uniform mixing and particle formation. Further pH of the reaction mixture was maintained slightly basic (pH 9). After the appearance of white precipitates at the bottom of flask, centrifuge the mixture at 10,000 rpm for 20 min, make sure the washing with distilled water and ethanol (Badar et al. , 2023).

Calcination and grinding of nanoparticles

Obtained particles were oven dried at 100°C for 1 hour, and then these NPs were calcinated at 400°C for 1 hour (Wu et al. 2011), followed by their grinding into a fine powder by using a mortar and pestle and stored (with date of synthesis) for further use.

Characterization of Nanoparticles

Prepared nanoparticles were further characterized by

- Ultraviolet-visible spectroscopy
- Fourier transform infrared spectroscopy
- X-ray diffraction Anlysis
- Scanning electron microscopy Analysis

Ultraviolet-Visible Spectroscopy analysis

Synthesized nanoparticles were first assessed through UV-Vis spectrophotometer analysis using spectrophotometer (Shimadzu UV-1800). Stock solution of NPs was prepared by dissolving 10mg ZnO NPs in 10mL deionized water in a glass beaker which was left on stirring till complete dispersion. Prepared stock solution was used for the analysis by taking this sample in a quartz cuvette. The wavelength of the instrument was kept in the range of 200-800 nm, while the scan speed was adjusted medium, and readings were recorded. UV vis analysis was performed for the confirmation of size, shape, and concentration of nanoparticles (Shamhari et al. 2018).

Fourier Transform Infrared Spectroscopy (FT-IR) Analysis

FTIR analysis was used to determine the functional groups present on the surface of ZnO NPs, ZnO NPs were mixed with potassium bromide (KBr) at a fixed ratio of 1:19. Prepared samples were then placed in a metal hole which was compressed until it was firmly packed, for this analysis FT-IR spectroscopy (Thermo Scientific) was used. This technique is essential for the detection of present functional groups on the surface of particles (Yang et al. 2009; Docter et al. 2015).

X-ray Diffraction (XRD) analysis

X-ray diffraction pattern of the dried biofabricated ZnO NPs were carried out using PANalytical Xpert powder diffractometer (Malvern) for the determination of shape and average size of green nanoparticles. The average crystallite size of biofabricated ZnO NPs was determined from the highest intense/narrower peak using Debye Sherrer's equation: $D=k\lambda\beta\cos\theta$
Where, D is crystallite size of nanoparticles, k is Sherrer's constant, which is 0.94, λ is the wavelength of X-ray sources used in XRD (1.5406Å), β is full width at half maximum (FWHM) of diffraction peak. θ refers to Bragg's angle. The most intense

peak was chosen which is <010> and crystalline size of synthesized `biofabricated ZnONPs was determined around 21.63 (Gholamali, I., & Yadollahi, M. (2021)).

Scanning Electron Microscopy (SEM) and EDX analysis

For further confirmations SEM analysis of prepared nanoparticles was performed using Carl Zeiss (model: FE-SEM sigma 500 VP) to assess the surface morphology, shape, and size of biofabricated ZnO NPs (Dihom et al., 2022).

RESULTS

Identification and classification of plant

Plant has been identified as *Pinus roxburghii* L. and saved in herbarium with botanical number of GC.Herb.Bot. 3754, Figure 1).

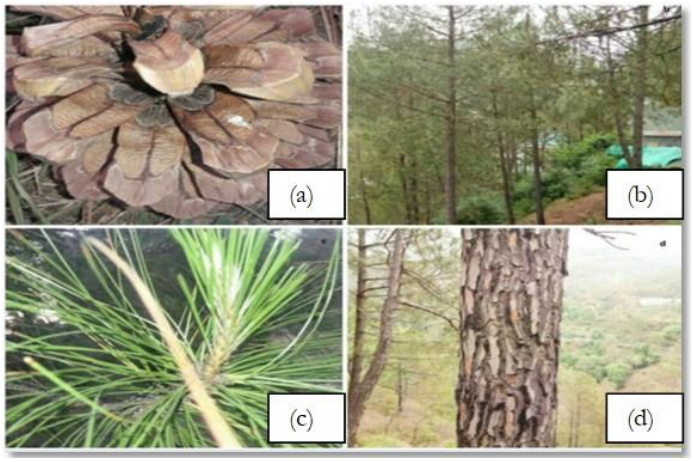

Kingdome: Plantae

Division: Tracheiophyte

Class: Pinopsida

Order: Pinales

Family: Pinaceae

Genus: Pinus

Species: Roxburghii

Figure 1 Characteristic features of *Pinus roxburghii* L. (a) Cone b) Tree c) Needles d) Trunk.) (Khan et al. , 2023)

Synthesis of Zinc oxide nanoparticles

A visual change in color of the reaction mixture was the first clear indication of the synthesis of ZnO NPs (Figure 2 A and B). A clear white colored powder of NPs were collected in glass petri plates after centrifugation.

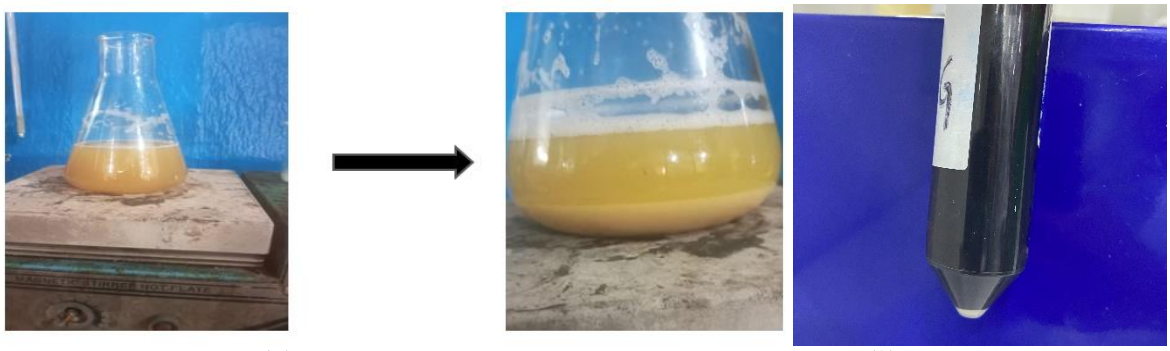

(A) (B)

Figure 2 Confirmation of synthesis of ZnO NP (A) Change in color (B) ZnO NP in solid form

Ultraviolet-Visible Spectroscopy analysis

A sharp and clear peak was detected at 377 nm which was an indication of zinc oxide nanoparticles (Figure 3 A and B). This peak was due to the surface plasmon response (SPR) effect, which is a collective oscillation of electrons at the surface of the NPs.

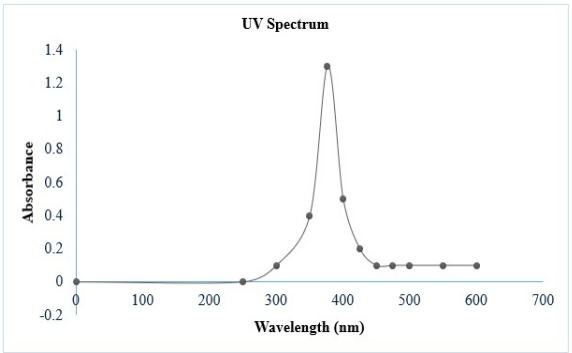

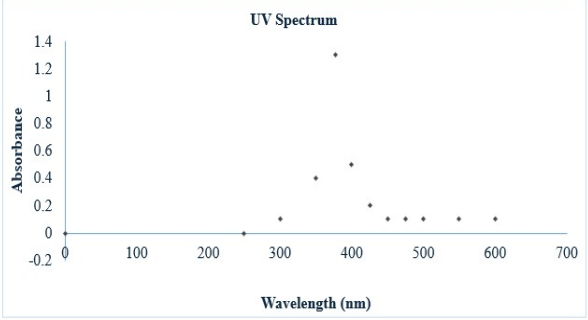

(A) (B)

Figure 3 UV Spectrum of bio -fabricated ZnO nanoparticles (A) Graphical presentation (B) Dotted presentation

Fourier Transform Infrared Spectroscopy (FT-IR) Analysis

Figure 4 clearly indicated the presences of carbon carbon double bonds C=C which means alkenes are present. Three sharp peaks at 1606 cm-1, 1953 cm-1 and 2115cm-1 were recorded which indicated the presence of aromatic rings and alkenes. Peak position at 2115cm-1 was due to the presence of carbonyl functional group, which is common in ketones, aldehydes, or carboxylic acids. There are some other possible compounds which may exhibit these peaks such as Terpenes, oleic acid, linoleic acid, acetone, methyl ethyl ketone, formaldehyde, acetaldehyde and acetic acid, propionic acid (Table 2).The peak at position detected at 2079 cm-1 was due to the presence of a nitrile functional group, which is common in compounds containing a cyano group (-CN). While peak at 1826cm-1indicated the presence of a carbonyl functional group, which is linked with ketones, aldehydes, or carboxylic acids. Similar peaks 1606 cm-1, 1953 cm-1 and 2115cm-1were recorded by the NPs prepared using *P. roxburghii* L. which is the indication of plant extract.However,two peaks were not recorded by NPs such as1826cm-1 and 2079cm-1which means some of the were break during nanoparticle synthesis, and some compounds reduced to form NPs. Presence of these stretches attributed to the zinc oxide nanoparticles.

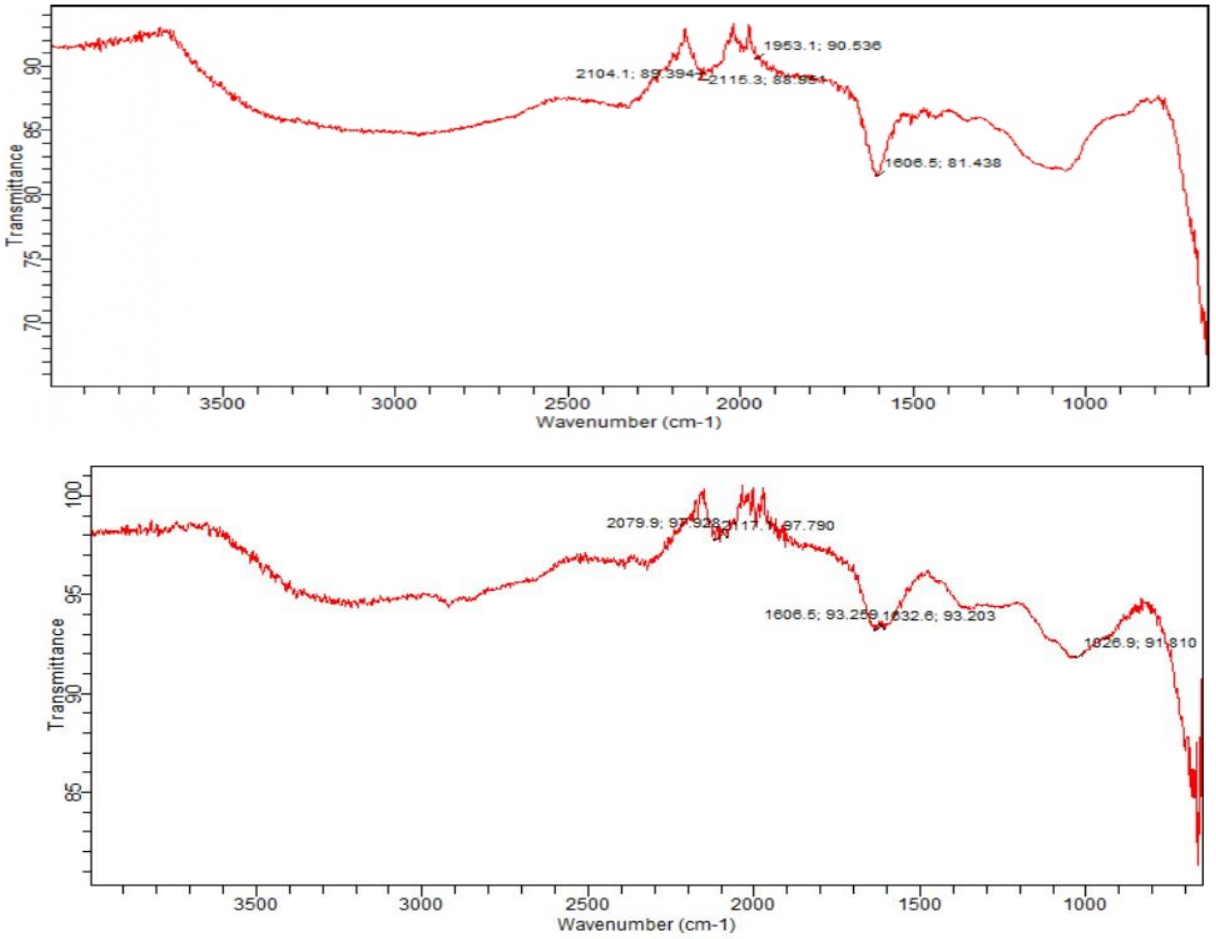

Figure 4 FTIR spectrums of bio-fabricated ZnO nanoparticles

Table 2.0 Identified functional groups after FTIR analysis of zinc nanoparticles

Plant extract		**ZnO NPs**	
Peak position	**Functional group**	**Peak position**	**Functional group**
1606 cm-1	C=C stretching (aromatic rings)	1606 cm-1	C=C stretching (aromatic rings)
1632 cm-1	C=N stretching vibration	1953 cm-1	C=C stretching (alkenes)
1826 cm-1	C=O stretching carbonyl functional group	2115 cm-1	C=O stretching carbonyl functional group
2117 cm-1	C=O stretching carbonyl functional group		
2079 cm-1	(C≡N) stretching vibration		

XRD analysis

The crystalline structure and phase of the nanoparticles (NPs) were characterized by X-ray diffraction (XRD) analysis, and the obtained results are presented in Figure 5. The XRD pattern of the ZnO NPs exhibited distinct peaks at (100), (002), (101), (102), (110), (103), (200), correspond to the hexagonal (wurtzite) structure of ZnO with preferred orientation along (101) plane. For the doped material, the XRD pattern showed 2θ=20.81°, 2θ=28.85°, 2θ=48.99° and 2θ=58.13° indexed.

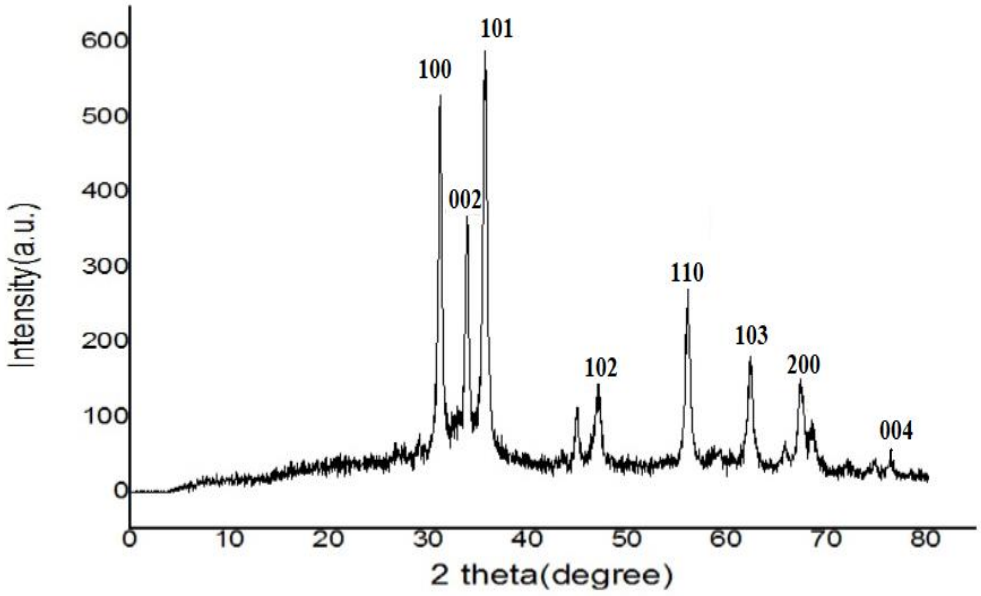

Figure 5 XRD patterns of ZnO NPs synthesized from the aqueous extract of *P. roxburghii* L. leaf

SEM Analysis

The SEM analysis revealed that the morphology and sized of biosynthesized ZnO NPs obtained as irregular in shape, well dispersed, uniform in size and well crystalline in nature. particle sizes ranging from 10 to 50 nm and a mean size of 24.71 nm (Figure 6 A-E).

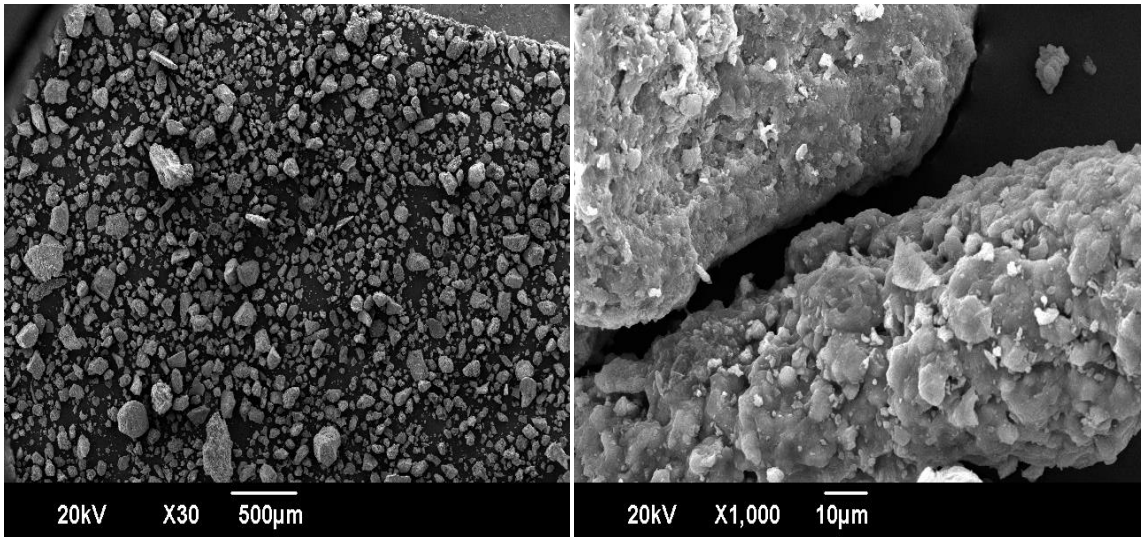

(A) (B)

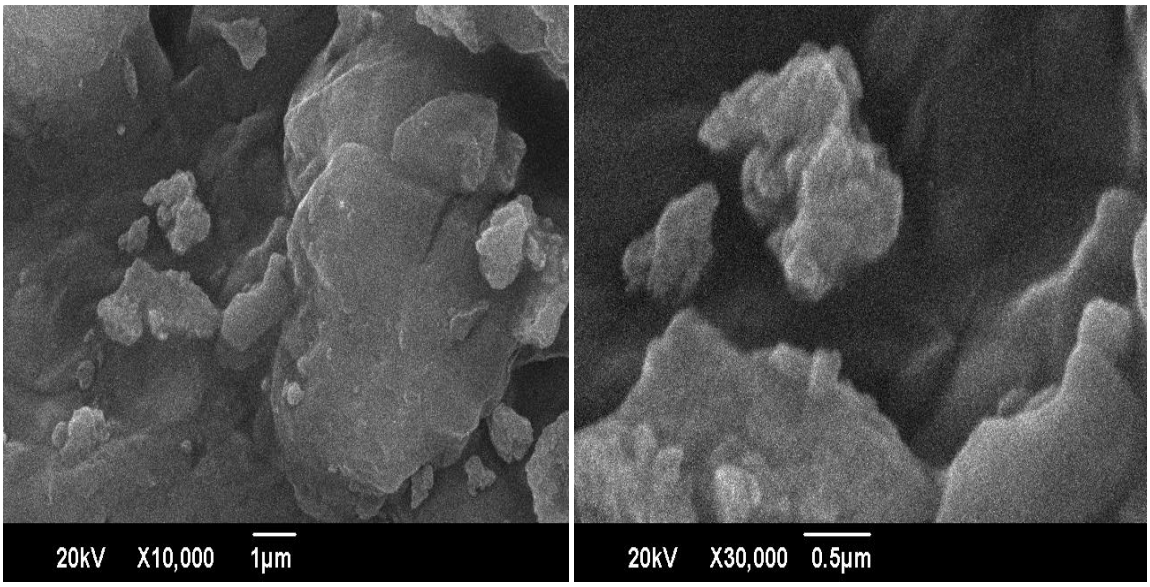

(C) (D)

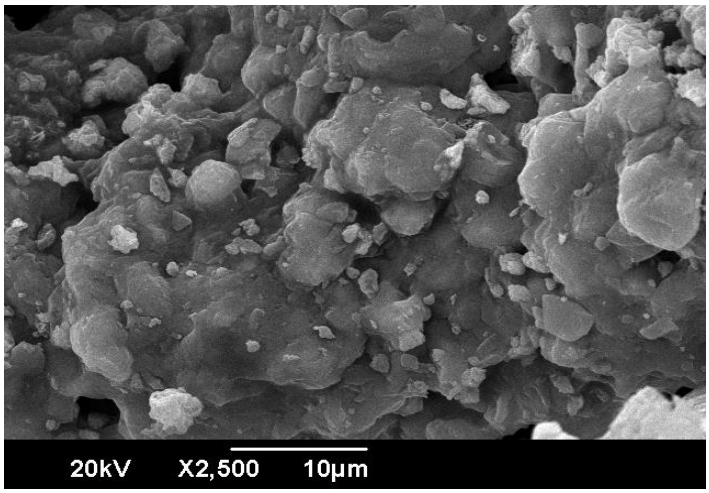

(E)

Figure 6 Scanning Electron Micrographs of ZnO NPs from *P. roxburghii* L. leaf extract at 20 kV

(A) X30 and 500 µm **(B)** X1000 and 10 µm **(C)** X10, 000 and 1.0 µm **(D)** X30, 000 and 0.5 µm **E)** X2500 and 10 µm

EDX Analysis

The elemental compositions of Zn ONPs were as present in prepared material, which yields strong to weak signals of 62.4% for zinc and 37.3% for oxygen (Figure 7), which is consistent with previous work on the synthesis of ZnO NPs.

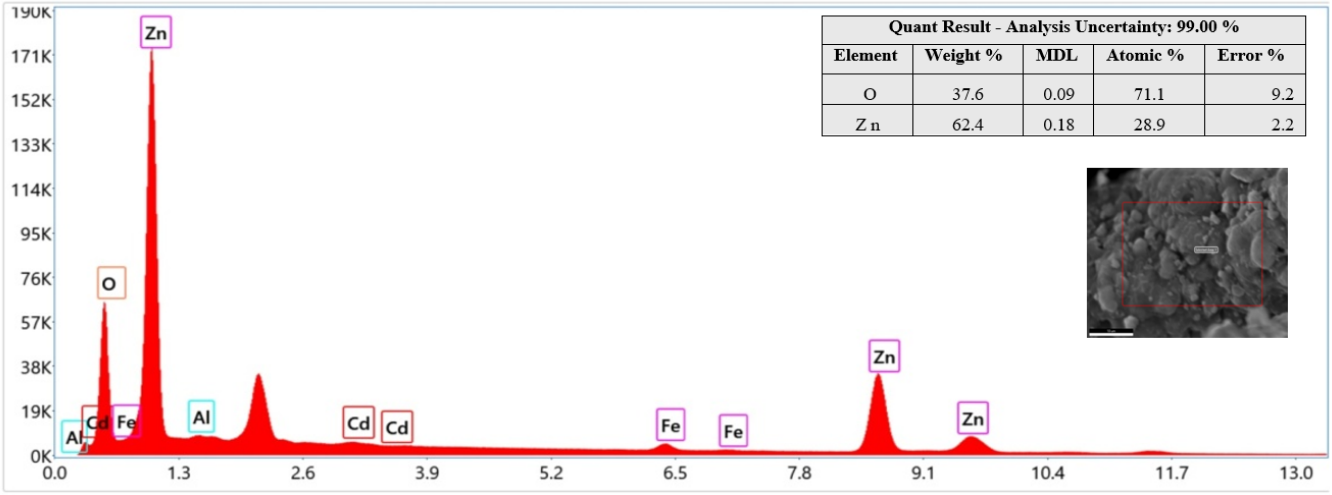

Figure 7 EDX analysis of ZnO NPs from *P. roxburghii* L. leaf extract

DISCUSSION

Visual observation of solution color change is the first indication of successful synthesis of nanoparticles (Happy et al. 2019). Reading of UV- vis in the wavelength range of 250–500 nm is used to assess the size of particles. In case of ZnO NPs maximum absorption had been found in the range of 300–350 nm (Nagajyothi et al. 2014). UV-vis analysis of ZnO NPs usually show a characteristic peak around 350-380 nm, a study conducted by Geetha and Sakthi, 2016 reported peak of ZnO NPs at 376 nm by UV analysis. Findings of study conducted by Asady et al (2020) were closely in favor with present study.

The presence of aromatic compounds in the *P. roxburghii* were found responsible for the synthesis of ZnO NPs similar findings were reported by Colak et al. (2017). Likewise, the peak positions attributed to carbonyl compounds were due to the used plant extract which has potential of catalytic activity of metal particles (Anusuya et al. 2021). The presence of flavonoids such as quercetin, kaempferol, and isorhapontigeninin the plant extract of *P. roxburghii* assisted synthesis of ZnO NPs (Bhuyan et al. 2015). Phytochemicals present in plant parts are the important constituents for the synthesis of nanoparticles. It had been reported that phytochemicals like flavonoids, ketones, aldehydes, amine, amide, organic acid are the key components for the reduction of Zinc ion to nanoparticles (Happy et al. 2019). Moreover this plant is also reported to have Abietadiene, Copaene, Humulene, Italicene, Juvabione, Sandaracopimarinal, Sclarene and Carene (Hasan et al. 2023) which are expected to be attached as a reducing agent with zinc nanoparticles.

Peak positions obtain in X-ray diffraction analysis by experimental samples were also reported by number of studies as in a study conducted by Demissie et al., (2020), diffraction peaks at 2θ value of ≈31.76°, 34.42°, 36.24°, 47.54°, 56.59°, 62.86°, 66.41°, 67.97°, and 69.06° were corresponding to (100), (002), (101), (102), (110), (103), (200), (112), and (201) crystal planes. Results of current study are in accordance to the results of present experimental analysis (Getie et al., 2017; Gholamali and Yadollahi, 2021). Results of another study suggested that sharp peaks obtained by XRD analysis were used to calculate average size. Reported results of another study were in line with present study suggested that NPs were hexagonal wurtzite in shape (Dobrucka and Dlugaszewska 2016).

SEM analysis was used for the morphological study of the experimental nanoparticles, as reported by experts (Rajiv et al., 2013).

CONCLUSION

Leaf extracts of *P. roxburghii* were an outstanding material for the synthesis of zinc oxide nanoparticles as this extract lead to the stability of nanoparticles and caping agents. Moreover, prepared nanoparticles were in nano range, while FTIR analysis revealed that the stability and the successful synthesis of these nanoparticles were due to different metabolites in plant extracts. Average size calculated was around 24.71 nm with irregular shape of particles. These nanoparticles could be further used for various branches of science due to their valuable features and are applicable for all kinds of advanced studies.

CONFLICT OF INTERESTS

There are no potential conflicts of interest declared by author (s).

AUTHOR CONTRIBUTION

KK performed all experimental work as a part of her PhD project and wrote the 1st draft of manuscript. **AA** designed and supervised the whole project, Edited, revised, and gave final approval to this manuscript. **HAK** supported for the analysis of data and English editing services and give final shape to the article, **KA** provided her technical support for experimental work. **MNH and SAK** provided her logistic and technical support for the analysis of data.

FUNDING : Not applicable.

AVAILABILITY OF DATA AND MATERIALS: All presented data are original.

REFERENCES CITED

1. Badar, R., Ahmed, A., &Munazir, M. (2023). Wheat leaf rust control through biofabricated zinc oxide nanoparticles. Australasian Plant Pathol.https://doi.org/10.1007/s13313-023-00949-1.
2. Getie, S., Belay, A., Chandra Reddy, A. R., & Belay, Z. (2017). Synthesis and characterizations of zinc oxide nanoparticles for antibacterial applications. J Nanomed Nanotechno S, 8(004).
3. Bhardwaj, K., Sharma, R., Cruz-Martins, N., Valko, M., Upadhyay, N.K., Kuča, K. & Bhardwaj, P. (2022), Studies of Phytochemicals, Antioxidant, and Antibacterial Activities of Pinus gerardiana and Pinus roxburghii Seed Extracts. BioMed Research International, 2022.
4. Hou, J., Zhang, Y., Zhu, Y., Zhou, B., Ren, C., Liang, S. & Guo, Y. (2019), α-Pinene induces apoptotic cell death via caspase activation in human ovarian cancer cells, Medical Science Monitor: International Medical Journal of Experimental and Clinical Research, 25 (6631).
5. Khan, H. A., Ahmed, A. , Kiran, K. , Hafeez, S. , Badar, R. & Ahmad, S. (2023). Phytocompound-based drug discovery approach to explore the frostbite healing potential of Abietadiene isolated from Pinus roxburghii. Journal of Population Therapeutics & Clinical Pharmacology. 30 (17): 1968-1986.
6. Banumathi, B., Vaseeharan, B., & Ishwarya, R., (2017). Toxicity of herbal extracts used in ethno-veterinary medicine and green-encapsulated ZnO nanoparticles against Aedes aegypti and microbial pathogens. Parasitology research, 116(6), 1637-1651.

7. Benelli, G., Maggi, F., Pavela, R., Murugan, K., Govindarajan, M., Vaseeharan, B. & Higuchi, A. (2018). Mosquito control with green nanopesticides: towards the One Health approach? A review of non-target effects. Environmental Science and Pollution Research, 25(11), 10184-10206.
8. Bisht, M., Sekar, K., & Arya, D. (2019). Diversity, utilization pattern, threat status and conservation of medicinal plants in great Himalayan national park, Himachal pradesh, western Himalaya. APJR,1.
9. Dihom, H. R., Al-Shaibani, M. M., Mohamed, R. M. S. R., Al-Gheethi, A. A., Sharma, A., & Khamidun, M. H. B. (2022). Photocatalytic degradation of disperse azo dyes in textile wastewater using green zinc oxide nanoparticles synthesized in plant extract: A critical review. Journal of Water Process Engineering, 47, 102705.
10. Divya, M., Vaseeharan, B., Abinaya, M., Vijayakumar, S., Govindarajan, M., & Alharbi, N. S. (2018). Biopolymer gelatin-coated zinc oxide nanoparticles showed high antibacterial, antibiofilm and anti-angiogenic activity. Journal of Photochemistry and Photobiology B: Biology, 178, 211-218.
11. Docter, D., Westmeier, D., Markiewicz, M., Stolte, S., Knauer, S. K., & Stauber, R. H. (2015). The nanoparticle biomolecule corona: lessons learned–challenge accepted.Chemical Society Reviews, 44(17), 6094-6121.
12. Farooq, Z., Iqbal, Z., Mushtaq, S., Muhammad, G., Iqbal, MZ., Arshad, M. (2008). Ethnoveterinary practices for the treatment of parasitic diseases in livestock in Cholistan desert (Pakistan). J Ethnopharmacol. 118(2), 213-219.
13. Gholamali, I., & Yadollahi, M. (2021). Bio-nanocomposite polymer hydrogels containing nanoparticles for drug delivery: A review. Regenerative Engineering and Translational Medicine, 7, 129-146.
14. Ishwarya, R., Vaseeharan, B., Kalyani, S., & Banumathi, B. (2018). Facile green synthesis of zinc oxide nanoparticles using Ulva lactuca seaweed extract and evaluation of their photocatalytic, antibiofilm and insecticidal activity. Journal of Photochemistry and Photobiology B: Biology, 178, 249-258.
15. Jakaria, Md., Islam, M., Shariful, I, Md., Belal, Talu, M., Dhar, Clint, C., & Ibrahim, M. (2017). Thrombolysis Potential of Methanol Extracts from the Five Medicinal Plants Leaf, Available in Bangladesh. Pharmacologia.
16. Karthika, V., Arumugam, A., Gopinath, K., &Kaleeswarran, P. (2017). Guazumaulmifolia bark-synthesized Ag, Au and Ag/Au alloy nanoparticles: Photocatalytic potential, DNA/protein interactions, anticancer activity and toxicity against 14 species of microbial pathogens. Journal of Photochemistry and Photobiology B: Biology, 167, 189-199.
17. Mundekkad, D., & Cho, W. C. (2022). Nanoparticles in Clinical Translation for Cancer Therapy. International journal of molecular sciences, 23(3), 1685. https://doi.org/10.3390/ijms23031685
18. Narayan, N., Meiyazhagan, A., &Vajtai, R. (2019). Metal Nanoparticles as Green Catalysts. Materials (Basel, Switzerland), 12(21), 3602. https://doi.org/10.3390/ma12213602
19. Neme, K., Nafady, A., Uddin, S., & Tola, Y. B. (2021). Application of nanotechnology in agriculture, postharvest loss reduction and food processing: food security implication and challenges. Heliyon, 7(12), e08539. https://doi.org/10.1016/j.heliyon.2021.e08539
20. Rajiv, P., Rajeshwari, S., & Venckatesh, R. (2013). Bio-Fabrication of zinc oxide nanoparticles using leaf extract of Parthenium hysterophorus L. and its size-dependent antifungal activity against plant fungal pathogens. Spectrochimica Acta Part A: Molecular and Biomolecular Spectroscopy, 112, 384-387.
21. Safaeian, L., Zolfaghari, B., Assarzadeh, N., Ghadirkhomi, A. (2019). Antioxidant and Anti-hyperlipidemic Effects of Bark Extract of Pinus eldarica in Dexamethasone-induced Dyslipidemic Rats. J Adv Med Biomed Res. 27(125), 49-56.
22. Sajid, A., Manzoor, Q., Iqbal, M., Tyagi, AK., Sarfraz, RA., Sajid, A. (2018). Pinus roxburghii essential oil anticancer activity and chemical composition evaluation. EXCLI J. 17,233-245.
23. Salem, MZM., Ali, HM., Basalah, MO. (2014). Essential Oils from Wood, Bark, and Needles of Pinus roxburghiiSarg. from Alexandria, Egypt: Antibacterial and Antioxidant Activities. Bioresources. 9(4), 7454-7466.
24. Secim-Karakaya, P., Saglam-Metiner, P., Yesil-Celiktas, O. (2021) Antimicrobial and wound healing properties of cotton fabrics functionalized with oil-in-water emulsions containing Pinus brutia bark extract and Pycnogenol® for biomedical applications. Cytotechnology, 73(3):423- 431.
25. Shamhari, N. M., Wee, B. S., Chin, S. F., & Kok, K. Y. (2018). Synthesis and Characterization of Zinc Oxide Nanoparticles with Small Particle Size Distribution. Acta ChimicaSlovenica, 65(3).
26. Shankar, Devkota, S., Paudel, K. (2015). Investigation of antioxidant and anti-inflammatory activity of roots of Rumex nepalensis. WJPPS. 4, 582-589.
27. Sharma A, Khanna S, Kaur G, & Singh I. (2021). Medicinal plants and their components for wound healing applications. Future Journal of Pharmaceutical Sciences; 7(1), 1-13.
28. Sharma, A., Sharma, L., Goyal, R. (2020). GC/MS Characterization, in-vitro Antioxidant, Antiinflammatory and Antimicrobial Activity of Essential Oils from Pinus Plant Species from Himachal Pradesh, India. JEOBP. 23(3), 522-531.
29. Singh, T., Jyoti, K., Patnaik, A., Singh, A., Chauhan, R., &Chandel, S. S. (2017). Biosynthesis, characterization and antibacterial activity of silver nanoparticles using an endophytic fungal supernatant of Raphanussativus. Journal of Genetic Engineering and Biotechnology, 15(1), 31-39.
30. Wu, C. M., Baltrusaitis, J., Gillan, E. G., &Grassian, V. H. (2011). Sulfur dioxide adsorption on ZnO nanoparticles and nanorods. The Journal of Physical Chemistry C, 115(20), 10164-10172.
31. Yang, K., Lin, D., & Xing, B. (2009). Interactions of humic acid with nanosized inorganic oxides. Langmuir, 25(6), 3571-3576.